A Numerical Investigation of Thermal and Mass Exchange of Blood Along Porous Stenosis Arterial Flow With Applied Magnetic Field

G. Shankar and E.P. Siva*

***Abstract*—Hemodynamics in stenosed arteries is complex, including turbulence, recirculation, and vortices, which can further worsen the disease. This study provides an overview of blood flow characteristics in stenosed arteries, focusing on flow physics, stenosis geometry, and severity. This present article examines the impact of heat and mass exchange on blood flow in arterial stenosis, taking into account chemical processes, magnetic fields, and thermal radiation. The features of vital fluid (blood) in the constricted arterial tube are examined by taking blood as Newtonian fluid in the arterial stenosis region. The continuity (mass), momentum, and concentration equations are solved using a finite difference approach with the help of appropriate boundary conditions. Solutions have been established for axial velocity, temperature, and concentration equations with variable parameters in blood circulation. It is noticed that an enhancement in the Reynolds number indicates more disorder in the velocity of the blood flow near the downstream area of cholesterol or plaque deposition. The temperature profile induced is stronger nearer to the arterial complaint wall downstream of stenosis. These findings for RBC's flow in stenosis-contained arteries have significant advantages in terms of understanding the disease mechanisms, developing accurate computational models, and identifying effective treatment strategies for patients.**

***Index Terms*—Blood flow; Concentration profile; Influence of mass and heat transfer; Magnetic; Mathematical modelling; Porous and radiation parameters.**

I. Introduction

THE discussion of blood movement through an artery accompanied by stenosis plays a significant role in many cardiovascular diseases. The character of blood depends on the hematocrit level where the whole red blood cells are occupied. The level of hematocrit in blood flow defines the relationship as the value of artery diameter reduces, and the RBC's level in the stenosed artery also reduces, as observed by the Fahraeous effect. Stenosis is an important factor in the cause of death in various cases. Stenosis is nothing but the narrowing of blood vessels or various tubes in the human body. Due to such narrowing, the blood flow in blood vessels thickens and causes diseases that, in severe cases, lead to death. The accumulation of fat and propagation of connective nerves in an arterial stenosis wall lead to the formation of plaques, which grow inward and restrict blood movement in the human body. In the cardiovascular system, the system transports nutrients and unused products from one part of the body to the other. The main function of the system is to provide oxygenated blood to every tissue over the arteries; thus, sufficient vital fluid blood rotation is required. If the blood gets thickened due to stenosis, the function is not performed properly, and so it causes severe arterial diseases. Leading causes of death due to heart dysfunction such as atherosclerosis, arteries becoming stenosed, and the hardening of tissues due to the formation of plaque and cholesterol.

The variety in the red blood cell region and how it affects the blood's rheological characteristics, including yield stress, are considered through two different approaches. One is collected from healthy and unhealthy donors, and the next is washing red cells a different number of times in saline, as investigated experimentally by Cokelet [1]. Young [2] discovered the impact of a time-varying blockage (stenosis) on the flow of fluid inside a tube. Vitro models (experimental) for separated flow can occur in the downstream areas, as explained by Young and Tsai [3]. Haldar [4] says that narrowing can take on different shapes, and this study is interested in understanding how these different shapes will impact blood flow resistance through the artery. Additionally, non-Newtonian and Newtonian blood flowing inside tapered arteries containing stenosis depositions was inspected by Misra [5] and Chakravarty [6]. Therefore, it seems that the effects of vessel tapering and stenosis shape on flow characteristics are equally significant and thus call for special consideration. David et al. [7]- [9] discovered the flow properties of blood are affected by factors and the presence of obstructions or constrictions in the blood vessels. They explained the circulatory system and physical behaviour of blood flow in arteries and veins, microcirculation, analogue models, and the finite difference scheme to solve the chosen governing equations. This study examines the pulsatile nature of the flow through arteries, which generates a dynamic environment that forms as a result of many interesting and fundamental unsteady fluid mechanics questions. Ponalagusamy [10] and Mishra et al. [11] studied two-layered models and composite types of stenosis, which are made up of different layers and can affect the performance of blood flow as it passes through.

Magnetohydrodynamics (MHD) is the study of the movement of conducting fluids through the effect of a magnetic field. If a magnetic field is applied to the conducting fluids, it conducts electricity and induces electric and magnetic fields. Bhavya et al. [12] analysed the influence of temperature distribution on blood flow over an inclined

Manuscript received July 13, 2023; revised January 04, 2024. G.Shankar is a research scholar, Department of Mathematics, College of Engineering and Technology, Faculty of Engineering and Technology, SRM Institute of Science and Technology, SRM Nagar, Kattankulathur-603203, Chengalpattu District, Tamil Nadu, INDIA (e-mail:sg1710@srmist.edu.in).

*E.P.Siva is an Associate Professor at Department of Mathematics, College of Engineering and Technology, Faculty of Engineering and Technology, SRM Institute of Science and Technology, SRM Nagar, Kattankulathur-603203, Chengalpattu District, Tamil Nadu, INDIA (corresponding author to provide email:sivae@srmist.edu.in).

porous stenosed artery with heat. Additionally, they assumed that the viscosity of blood varies with hematocrit, specifically within the artery region.

The radiation effect in human blood has a significant role in treatments. The radiation affects the cancerous tissues by overheating them with electromagnetic radiation. The procedure involves the transmission of heat over the affected area through the surface of the skin into the tissues and muscles. By heating them to high temperatures, they speed up healing by increasing blood flow. Sinha et al. [13] theoretically analysed the magnetohydrodynamic flow of vital fluid in capillaries and analysed the effect of temperature and velocity of the blood. Chakravarty and Mandal [14] have discussed the character of the blood flow and found the behaviour of streamlines, flow velocity, pressure drop, and Wall Shear Stress (WSS). They have also found that temperature and concentration have less influence on unsteady blood movements in irregularly multi-stenosed arteries. Sreeparna and Shit [15] have explained the disparity of the velocity along the radial track with distinct values of the parameter and at dissimilar places of the stenosed artery. Also, the condition of the stenosed artery plays a significant role in the influence of the parameter. The parameter calculates the value in accordance with the velocity, viscosity, pressure, length of the blood vessel, or arterial difference obtained by the difference in these aspects in the stenosed region. Tashtoush and Magableh [16] conducted a study on the influence of magnetic fields on the geometry of arteries with multiple stenoses. Moreover, the heat transfer acts by inducing a static magnetic field. Prakash and Makinde [17] studied the heat transmission to fluid movement over the stenosis artery in the presence of MHD. The literature survey [18]-[20] reports the effect and the factors that affect the blood flow in arterial stenosis. The unsteady flow of blood over the arterial stenosis with radiative heat transfer, magnetic field, pressure gradient, and velocity profile is studied. Nadeem and Ijaz [21] concluded that the resistance impedance and the flow and pressure difference both give the best results for converging and diverging tapering, respectively.

Yadong [22] and Mekheimer et al. [23] investigated the mixed convection influence of thermal (heat) and mass transfer in 2D pulsatile and micropolar blood flow through a tapered stenosed artery. Yadong observed the velocity profile of blood and gave valuable suggestions on heat and mass transfer. The natural convection of temperature and concentration of a couple stress fluids with silver nanoparticles through tapered stenosed arteries is explained by Ramana et al. [24]. It has been shown that the Nusselt number is directly proportional to the volume fraction and enhances molecular heat dispersal by increasing the concentration of nanoparticles. Nadeem [25] and Umadevi et al. [26] explained metallic and mixed copper water-based nanofluid inside a curved artery with the presence of a permeable wall and magnetic field. Umadevi concluded that Cu-water has higher flow resistance than pure water due to copper-enhancing artery flexibility. Ponalagusamy and Priyadharshini [27]-[29] analyzed two types of fluid (plasma and micropolar) in the peripheral layer through a tapered stenosed artery and extended their research with the help of a variable magnetic field and acceleration of the periodic body. They found the trapping bolus size is increasing in couple stress fluid compared to Newtonian fluid. Furthermore, hematocrit and WSS are directly proportional to each other. A 2D rheological blood flow model in a tapered diseased stenosis artery was solved by using the finite element method, which was explained by Dubey and Vasu [30]. Also, consider the blood flow model, Eringen micropolar. They reveal that the pulsatile parameters have the opposite behaviour as WSS. Ameenuddin et al. [31] modeled a set of non-linear governing equations indicating the variations in shear rate and the concentration of hematocrit level in human blood.

Model of K.L. fluid blood flow in a constricted tapered artery without a slip condition on the wall and time-dependent constriction discussed by Ponalagusamy [32]. The K-L model was compared to both Newtonian and non-Newtonian fluids in terms of velocity field, wall shear stress, and resistive impedance. They discovered that the flow properties of K-L fluid differ from those of Casson fluid depending on the values of the K-L fluid parameters used. Prasad et al. [33] analysed the unique properties of blood flow in a specific type of artery (porous tapered artery) with mild stenoses, particularly focusing on how an external magnetic field affects this flow. Furthermore, it was found that as the speed of the applied magnetic field increases, the shear stress also rises accordingly. Conversely, when there is an increment in the permeability parameter, the shear stress decreases. The influence of both variable and constant viscosity on the Bingham plastic blood model, along with the transverse magnetic field in tapered arteries, was discovered by Veena [34] and Devaki et al. [35]. They came to the conclusion that when the Womersley number is high, the rate of change in the volumetric flow rate inside the artery is lower over time. Increasing the Darcy number can improve the flow rate at the beginning and end of stenosis, but there were no significant changes in wall shear stress when the Womersley number was high. Bhavya and Sharma [36] studied the influences of varying viscosity on arterial blood flow within inclined arteries under the influence of a magnetic field while considering the presence of chemical reactions. As a result of this impact, strong magnetic field intensity will create plaque rupture, which can harm the body by paralysing the affected area. Pulsatile blood flow through an elastic artery with the introduction of a uniform magnetic field was described by Sadeghi et al. [37] and Kumar [38]. They reveal that the magnetic field has a larger effect on single stenosis than on double stenosis. For maximum velocities, the effects of the Hartmann number (Ha) on the artery wall shear stress in the region affected by both single and multiple stenoses indicate that an increasing Hartmann number increases shear stress. Gudekote et al. [39] and Buzuzi [40], and Shankar & Siva [41] investigated the influence of heat and mass transfer on the peristaltic movement of an Eyring Powell and non-uniform MHD Casson and Williamson fluid through an inclined channel. Sweed et al. [42] and Das et al. [43] explained the pulsatile blood and EMHD flow in asymmetric and inclined channels, respectively.

Considering the aforementioned discussion, our proposed study aims to explore the blood flow in a stenosed artery of a Newtonian fluid in the presence of a magnetic field, chemical reaction, thermal radiation, radiative heat flux, and porous medium. Solutions have been established for the axial velocity, temperature, and concentration equations of

the blood flow inside an artery. To learn the characteristics of blood flow, the velocity profile, temperature profile, porous parameter, radiation parameter, and concentration profile have been depicted for various ranges of magnetic parameters.

II. Mathematical Modeling

In this current paper, we discuss the application of permeability (porous medium) for the learning of vital fluid movement through the arterial stenosis in the occurrence of MHD. The application of MHD to physiological problems is gaining attention. Consider the model of incompressible vital fluid flow through an arterial stenosis of stretch L. Moreover, let us consider the cylindrical stenosed artery with a radius of $\bar{r}$, whereas the viscosity of the fluid is $\bar{\mu}$. The fluid flow can be organised by smearing enough of a magnetic field. Let the blood flow axis be considered as $\bar{z}$. The channel is supposed to be of cylindrical shape since the blood flow in the artery is pipe flow in nature, with $(\bar{u}, \bar{v}, \bar{w})$ being the velocities along $(\bar{r}, \bar{\theta}, \bar{z})$ direction. Let $\bar{T}_w$ be the temperature of the outer wall and $\bar{C}_w$ be the concentration of the outer wall of the artery. The geometry of the arterial stenosis [2] is symmetric about the $\bar{z}$ direction, which is given by

$$\frac{\bar{R}(\bar{z})}{\bar{R}_0} = \begin{cases} 1 - \frac{\delta_0}{2\bar{R}_0}\left(1 + \cos\frac{2\pi}{L_0}\left(\bar{z} - \bar{d} - \frac{L_0}{2}\right)\right) & \text{for} \quad d_0 + L_0 \le \bar{z} \le d_0 + 4L_0, \\ 1\,, \text{ otherwise.} \end{cases} \tag{1}$$

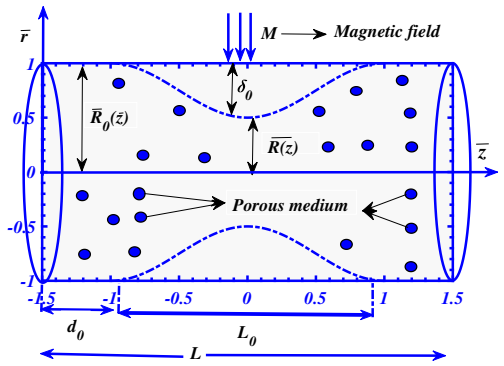

Fig. 1: Diagram of a stenosed artery

where L_0 is the stenosis length and d_0 the coaction of stenosis. $\bar{R}(\bar{z}), \bar{R}_0(\bar{z})$ are the stenosis radius and healthy artery radius, respectively. n decide the compression profile shape, and δ_0 specifies the extreme height of the arterial stenosis situated at

$$\bar{z} = d + \frac{L_0}{n^{\frac{1}{(n-1)}}}. \tag{2}$$

where n = 2 is the extreme height of the stenosis that arises in the middle part of the arterial area.

$$\bar{z} = d + \frac{L_0}{2}. \tag{3}$$

Since it is considered that the blood is a Newtonian incompressible fluid.

II-A. Governing Equations

The chosen governing equations of the fluid motion in the cylindrical coordinates $(\bar{r}, \bar{z})$ are given by [12]:

$$\bar{\rho}\frac{\partial \bar{u}}{\partial \bar{t}} = -\frac{\partial \bar{p}}{\partial \bar{z}} + \bar{\mu}\left(\frac{\partial^2 \bar{u}}{\partial \bar{r}^2} + \frac{1}{\bar{r}}\frac{\partial \bar{u}}{\partial \bar{r}}\right) - \frac{\bar{\mu}}{k_0}\bar{u} + \bar{\rho}\bar{g}\bar{\beta}\left(\bar{T} - \bar{T}_0\right) - \bar{\sigma}\bar{B}_0^2\bar{u} + \bar{\rho}\bar{g}\bar{\gamma}\left(\bar{C} - \bar{C}_0\right), \tag{4}$$

$$\bar{\rho}\bar{C}_p\frac{\partial \bar{T}}{\partial \bar{t}} = \bar{K}\left(\frac{\partial^2 \bar{T}}{\partial \bar{r}^2} + \frac{1}{\bar{r}}\frac{\partial \bar{T}}{\partial \bar{r}}\right) - \frac{\partial \bar{q}}{\partial \bar{r}}, \tag{5}$$

$$\frac{\partial \bar{C}}{\partial \bar{t}} = \bar{D}\left(\frac{\partial^2 \bar{C}}{\partial \bar{r}^2} + \frac{1}{\bar{r}}\frac{\partial \bar{C}}{\partial \bar{r}}\right) + \bar{E}\left(\bar{C} - \bar{C}_0\right). \tag{6}$$

where $\bar{B}_0$ is the applied magnetic field, $\bar{E}$ is the chemical reaction parameter, $\bar{\sigma}$ is the electrical conductivity, $\frac{\partial \bar{p}}{\partial \bar{z}}$ is the represents pressure gradient, $\bar{D}$ is the mass diffusivity, $\bar{\rho}$ is the density of the fluid, $\bar{C}_p$ is the specific heat, $\bar{K}$ is the thermal conductivity, $\frac{\partial \bar{q}}{\partial \bar{r}}$ is the radiation effect of heat transfer and $\bar{u}$ is the velocity of the blood flow in radial direction. Where $\bar{q}$ represents radiative heat flux in the region. To solve the velocity, heat, and mass equations of the blood using no-slip boundary conditions, which are measured in the artery. The boundary conditions are as follows

$$\begin{gathered} \bar{u} = 0, \ \bar{T} = \bar{T}_w \ \text{ and } \bar{C} = \bar{C}_w \ \text{ at } \ \bar{r} = \bar{R}(\bar{z}), \\ \frac{\partial \bar{u}}{\partial \bar{r}} = 0, \quad \frac{\partial \bar{C}}{\partial \bar{r}} = 0 \quad \text{and} \quad \frac{\partial \bar{T}}{\partial \bar{r}} = 0 \quad \text{at } \bar{r} = 0. \end{gathered} \tag{7}$$

II-B. Non-Dimensional Analysis and Approximations

Now we assume the following non dimensional parameters from [12]:

$$Re = \frac{\bar{\rho}\bar{R}_0^2\omega}{\bar{\mu}}, p = \frac{\bar{R}_0\bar{p}}{\bar{u}_0\bar{\mu}}, z = \frac{\bar{z}}{\bar{R}_0}, \ t = \bar{\omega}\bar{t}, R(z) = \frac{\bar{R}(\bar{z})}{\bar{R}_0},$$

$$\bar{E} = \frac{E\bar{\mu}}{\bar{\rho}\bar{R}_0^2}, r = \frac{\bar{r}}{\bar{R}_0}, u = \frac{\bar{u}}{\bar{u}_0}, \ \theta = \frac{\bar{T} - \bar{T}_0}{\bar{T}_w - \bar{T}_0}, \ N^2 = \frac{4\bar{R}_0^2\overline{\alpha}^2}{\bar{K}},$$

$$M^2 = \frac{\bar{\sigma}\bar{B}_0^2\bar{R}_0^2}{\bar{\mu}}, \sigma = \frac{\bar{C} - \bar{C}_0}{\bar{C}_w - \bar{C}_0}, \ Gr = \frac{\bar{\rho}\bar{g}\bar{\beta}\bar{R}_0^2\left(\bar{T}_w - \bar{T}_0\right)}{\bar{u}_0\bar{\mu}},$$

$$Gc = \frac{\bar{\rho}\bar{g}\bar{\gamma}\bar{R}_0^2\left(\bar{C}_w - \bar{C}_0\right)}{\bar{u}_0\bar{\mu}}; \ Pe = \frac{\bar{\rho}\bar{c}_p\bar{R}_0^2\bar{\omega}}{\bar{K}}; \ Sc = \frac{\bar{\mu}}{\bar{\rho}\bar{D}}.$$

The equation of velocity, heat and mass transfer equation of the cylindrical section in the dimensionless form is given by

$$-\frac{\partial p}{\partial z} + \left(\frac{\partial^2 u}{\partial r^2} + \frac{1}{r}\frac{\partial u}{\partial r}\right) + Gr\theta - \left(M^2 + \frac{1}{k}\right)u + Gc\sigma = Re\frac{\partial u}{\partial t}, \tag{8}$$

$$where \ k = \frac{k_0}{\bar{R}_0^2}.$$

$$p_e\frac{\partial \theta}{\partial t} = \left(\frac{\partial^2 \theta}{\partial r^2} + \frac{1}{r}\frac{\partial \theta}{\partial r}\right) - N^2\theta, \tag{9}$$

$$Re\frac{\partial \sigma}{\partial t} = \frac{1}{Sc}\left(\frac{\partial^2 \sigma}{\partial r^2} + \frac{1}{r}\frac{\partial \sigma}{\partial r}\right) - E\sigma. \tag{10}$$

The skin-friction coefficient (wall shear stress) is calculated using Eq. (11), while the thermal (heat) flux (rate of thermal

exchange) is calculated using Eq. (12).
The skin friction parameter on the wall is defined as

$$\tau_w = -\mu \left(\frac{\partial u}{\partial r}\right) \quad at \quad r = R \tag{11}$$

The local Nusselt number parameter is defined as

$$Nu = -\left(\frac{\partial \theta}{\partial r}\right) \quad at \quad r = R \tag{12}$$

The equation that describes the rate at which mass is transferred through the wall of the artery is given by

$$Sh = -\left(\frac{\partial \sigma}{\partial r}\right) \quad at \quad r = R \tag{13}$$

Where *N* is the thermal radiation, *E* is the chemical reaction quantity, and *M*, *k* are the magnetic and porous parameters, respectively. Applying the non-dimensional quantity in equation [1], the arterial stenosis is given by

$$R(z) = \begin{cases} 1 - \frac{\delta}{2}\left(1 + \cos 2\pi\left(z - d - \frac{1}{2}\right)\right), d_0 + 1 \le z \le d_0 + 4, \\ 1, \text{otherwise.} \end{cases} \tag{14}$$

III. Boundary Conditions

The dimensional boundary conditions are as follows:

$$\overline{u} = 0,\ \overline{T} = \bar{T}_w \ \text{ and } \overline{C} = \bar{C}_w \ \text{ at } \ \bar{r} = \bar{R}(\bar{z}),$$

$$\frac{\partial \bar{u}}{\partial \bar{r}} = 0,\ \frac{\partial \bar{T}}{\partial \bar{r}} = 0 \ \text{ and } \frac{\partial \bar{C}}{\partial \bar{r}} = 0 \ \text{ at } \ \bar{r} = 0.$$

The respective non-dimensional boundary conditions are given by

$$\begin{aligned} u = 0,\ \theta = 1,\ \sigma = 1 \quad \text{at} \quad r = R(z), \\ \frac{\partial u}{\partial r} = 0,\ \frac{\partial \theta}{\partial r} = 0,\ \frac{\partial \sigma}{\partial r} = 0 \quad \text{at} \quad r = 0. \end{aligned} \tag{15}$$

IV. Numerical Approach

The respective non-dimensional boundary condition let us first apply the finite difference discretization scheme to discretize nonlinear equations (8–10). We use the central difference approximations to solve the spatial derivatives and the explicit forward finite difference approximations to discretize the time derivative in the following manner are given by

$$u = \left[\frac{u_i^{n+1} + u_i^n}{2}\right], \frac{\partial u}{\partial t} = \left[\frac{u_i^{n+1} - u_i^n}{\Delta t}\right],$$

$$\theta = \left[\frac{\theta_i^{n+1} + \theta_i^n}{2}\right], \sigma = \left[\frac{\sigma_i^{n+1} + \sigma_i^n}{2}\right],$$

$$\frac{\partial u}{\partial r} = \frac{1}{2}\left[\frac{u_{i+1}^{n+1} - u_{i-1}^{n+1} + u_{i+1}^n - u_{i-1}^n}{2(\Delta r)}\right],$$

$$\frac{\partial^2 u}{\partial r^2} = \left[\frac{(u_{i+1}^{n+1} - 2u_i^{n+1} + u_{i-1}^{n+1}) + (u_{i+1}^n - 2u_i^n + u_{i-1}^n)}{2(\Delta r)^2}\right],$$

$$\begin{aligned} &-\frac{\partial p}{\partial z} + \left[\frac{(u_{i+1}^{n+1} - 2u_i^{n+1} + u_{i-1}^{n+1}) + (u_{i+1}^n - 2u_i^n + u_{i-1}^n)}{2(\Delta r)^2}\right] \\ &+ \frac{1}{2r}\left[\frac{u_{i+1}^{n+1} - u_{i-1}^{n+1} + u_{i+1}^n - u_{i-1}^n}{2(\Delta r)}\right] + Gr\left[\frac{\theta_i^{n+1} + \theta_i^n}{2}\right] \\ &- (M^2 + \frac{1}{k})\left[\frac{u_i^{n+1} + u_i^n}{2}\right] + Gc\left[\frac{\sigma_i^{n+1} + \sigma_i^n}{2}\right] \\ &= Re\left[\frac{u_i^{n+1} - u_i^n}{\Delta t}\right], \end{aligned} \tag{16}$$

$$\begin{aligned} Pe\left[\frac{\theta_i^{n+1} - \theta_i^n}{\Delta t}\right] &= \frac{1}{2r}\left[\frac{\theta_{i+1}^{n+1} - \theta_{i-1}^{n+1} + \theta_{i+1}^n - \theta_{i-1}^n}{2(\Delta r)}\right] \\ &+ \left[\frac{(\theta_{i+1}^{n+1} - 2\theta_i^{n+1} + \theta_{i-1}^{n+1}) + (\theta_{i+1}^n - 2\theta_i^n + \theta_{i-1}^n)}{2(\Delta r)^2}\right] \\ &- N^2\left[\frac{\theta_i^{n+1} + \theta_i^n}{2}\right], \end{aligned} \tag{17}$$

$$\begin{aligned} Re\left[\frac{\sigma_i^{n+1} - \sigma_i^n}{\Delta t}\right] &= \frac{1}{Sc}\left[\frac{\sigma_{i+1}^{n+1} - \sigma_{i-1}^{n+1} + \sigma_{i+1}^n - \sigma_{i-1}^n}{4r(\Delta r)}\right] \\ &+ \frac{1}{Sc}\left[\frac{(\sigma_{i+1}^{n+1} - 2\sigma_i^{n+1} + \sigma_{i-1}^{n+1}) + (\sigma_{i+1}^n - 2\sigma_i^n + \sigma_{i-1}^n)}{2(\Delta r)^2}\right] \\ &- E\left[\frac{\sigma_i^{n+1} + \sigma_i^n}{2}\right]. \end{aligned} \tag{18}$$

V. Results and Discussion

In this part, the effect of the velocity (u) profile, temperature distribution profile (θ), and concentration profile (σ) of the blood flow on various pertinent parameters has been elaborately discussed. In this segment, we collected measurements to see how different factors affect the thing we were looking into. porous parameter (*k*), Reynolds number (*Re*), magnetic influence (*M*), Grashof number (*Gr*), mass Grashof number (*Gc*), thermal radiation effect (*N*), Peclet number (*Pe*), Schmidt number (*Sc*), a chemical reaction (*E*), various heights of stenosis (δ), four separate time periods (*t*), and the profiles of velocity, temperature, and concentration are some of the things that these factors take into account. Additionally, we look at how stenosis acts in terms of speed and time.

Figures 2–17 show how these factors change things, and we explain in detail the significance of those changes. It includes four subsections in this part. The first part is all about looking at how the dimensionless axial velocity profile changes when certain factors are changed. In the parts that follow, we will discuss how different factors affect dimensionless temperature and concentration profiles, as well as how stenosis behaves. Table I provides the default settings for the parameters utilised in the graphical analysis of the model's efficacy. Tables II, III, and IV present the local skin friction, Nusselt number, and Sherwood number, respectively. These tables account for various parameters, such as the Reynolds number, magnetic field strength, porous parameter, thermal and mass Grashof numbers, Peclet number, and thermal radiation.

Table I. The values of the parameters [12].

Parameters	Values
Magnetic field parameter (M)	1-5
Grashof number (Gr)	1-6
Porous parameter (k)	0-1
Mass Grashof number (Gc)	1-6
Chemical reaction parameter (E)	0-2
Thermal radiation parameter (N)	2-10
Peclet number (Pe)	0-2
Schmidt number (Sc)	0-2
Eckert number (Ec)	0-2

Table II. Local skin friction.

Re	M	k	Gr	Gc	Skin friction
1	2.23	0.5	3	3	0.1037
2					0.1166
3					0.1203
4					0.1220
5	1.5	0.5	3	2	0.1386
	2.5				0.1365
	3.5				0.1331
	4.5				0.1285
5	2.23	0.2	3	3	0.1210
		0.5			0.1228
		0.7			0.1232
		1			0.1235
5	2.23	0.5	1	2	0.1231
			3		0.1240
			5		0.1249
			6		0.1259
5	2.23	0.5	3	1	0.0234
				3	0.0249
				5	0.0265
				6	0.0280

Table III. Local Nusselt number.

Pe	N	Nusselt Number
1	2.5	0.0337
2		0.0429
3		0.0459
4		0.0473
1.5	1	0.0403
	2	0.0363
	3	0.0288
	4	0.0203

Table IV. Local Sherwood number.

Sc	E	Re	Sherwood number
0.5	0.2	3	3.3876
1			2.4568
1.5			1.8185
2			0.5178
0.8	0	2	2.2884
	0.5		1.3827
	0.8		1.0221
	1		0.8356
1	1.5	2.5	4.7437
		3	2.5728
		3.5	1.5014
		4	0.9312

V-A. Flow Characteristics

Figures 2–6 show the effects of various parameters like magnetic field parameter (M), Grashof number (Gr), Reynolds number (Re), porous parameter (k), and mass Grashof number (Gc) on the velocity of the fluid flow. The velocity distribution in the axial direction of blood flow decreases with respect to an increase in the magnetic parameter (M). When blood flows through a magnetic field, erythrocytes align their disc plane parallel to the magnetic field's direction. This activity induces an increase in the internal blood viscosity by increasing red blood cell concentration. The variation in concentration of the haemoglobin molecule, which is made of iron content, is figured out against the magnetic field, which is depicted in figure 2. The blood flow under the influence of an applied magnetic field is directly proportional to the direction of the magnetic field (M). There is a downturn in the velocity profile of the fluid (blood) flow in stenosed arteries as the value of the applied magnetic field parameter increases. The stenosis plays a vital role in the increase and decrease of the chosen parameters. In the arteries, the creation of plaque or stenosis disturbs the blood flow rate. The geometry of stenosis affects the blood flow. Figure 3 explains the characteristics of the velocity profile of blood with the heat Grashof number. Elevated values of the thermal Grashof number are indicative of a substantial temperature gradient, which in turn generates a heightened buoyancy force responsible for propelling the fluid motion. The fluid experiences a greater buoyant force near the centre due to higher temperatures, whereas the force at the wall is comparatively smaller. It is noted that as the Grashof number increases, the velocity of blood flow increases. It is detected from Figure 4 that the behaviour of the velocity of blood has a Reynolds number. It is noted that as it increases, the velocity profile of blood flow decreases. The enhancement of stress increases the potency of the magnetic field. The streaming blood affects the flexibility of the wall, which results in an increase in pressure. We observe that an increase in Re causes more disorder in fluid (blood) velocity at the downstream of the area of cholesterol or panel deposition, and the temperature induced is strong near the arterial wall at the downstream of stenosis. Figure 5 indicates the variation of the permeability parameter with the velocity of blood. It reveals that with an increase in the permeability parameter, the velocity profile of blood flow enhances. Figure 6 shows a profile of the velocity of blood with a mass Grashof number. It is detected that as the mass Grashof number rises, the velocity of blood flow increases.

V-B. Thermal Characteristics

The temperature profile in a stenosed artery can be affected by the Peclet number because the convective transport of blood can cause a significant mixing of heat in the fluid, while the diffusive transport of heat is much slower. This can result in a non-uniform temperature distribution in the fluid, with a higher temperature near the core region of the artery and a lower temperature near the wall. Figures 7 and 8 show a profile of the temperature of the blood with thermal radiation and the Peclet number, respectively. It is seen from Figure 7 that as the thermal radiation increases, the temperature decreases. The temperature of the blood along

the radial coordinates does not impact the blood flow. The temperature in the stenosed artery does impact the thermal radiation, which leads to a decrease in thermal radiation. It is shown in Figure 8 that the Peclet number increases with a decrease in temperature; this is due to heat transfer and the thermal energy in the blood. For the values in the Peclet number, the heat transfer in the blood causes the temperature to decrease in the blood flow. The benefits of thermal radiation in blood flowing inside the diseased artery include its non-invasive, safe, and painless nature, accurate measurements, early detection, and cost-effectiveness. These benefits can lead to better diagnosis and treatment outcomes for patients with blood flow diseases of the artery.

V-C. Concentration Profile

The concentration of the blood suppresses due to mass diffusivity in the blood. It is noted from figures 9–10 that both the Schmidt number *(Sc)* and chemical reaction parameter (E) increase with a decrease in the concentration of blood flow in the arterial stenotic region. This phenomenon could be observed as the buildup of specific substances (reactants) and decreased levels of products, potentially impacting the general physiology and functionality of the circulatory system and the tissues it supplies. Figures 9 and 10 concluded that both the chemical reaction parameter and Schmidt number have a direct impact on the concentration profile, with an increase in either of them leading to a decrease in the species concentration in the fluid. In the case of blood flow in an artery that has narrowed, a smaller Schmidt number could mean that solutes spread out better and that substances are more evenly spread in the blood. This could be because mass diffusion is working better, so there are fewer sharp variations in concentration and the concentration curve is smoother.

V-D. Behaviour of Stenosis

Figure 11 demonstrates a clear inverse relationship between the height of the stenosis δ and the axial velocity, indicating that a rise in δ leads to a decrease in axial velocity. In more accessible language, as the stenosis of an artery increases, the axial blood flow velocity decreases. The reduction in velocity can have significant implications for hemodynamics and general perfusion inside the affected arterial location. Figure 12 shows the results of the radial velocity components changing over four different time periods when the narrowing of the artery is at its worst. These flow speeds, on the other hand, are always positive. They start at zero on the axis and build as you move away from it until they reach a fixed value on the artery wall surface. It looks like all of the shapes are sloping towards the wall, which means they are open to nonlinear flow. In clinical settings, it is very important to know how pressure differences affect the speed of blood flow in vessels that are narrowed. It helps doctors figure out how bad arterial blockages are and plan the right treatments, like angioplasty (a procedure to open up narrowed or blocked arteries) or stent placement, to get blood flowing normally again and avoid problems like thrombosis, embolism, or ischemia. Figure 13 depicts the relationship between blood flow velocity and radial distance (r) under different pressure gradients. The velocity (u) exhibits a negative correlation with the radius of stenosis, such that an increase in the radius of stenosis leads to a drop in velocity. Based on the Hagen-Poiseuille equation, it can be observed that a slight increase in the radius leads to a substantial increase in the flow rate, under the condition that other variables, such as the viscosity and length of the vessel, remain unchanged. The rate of blood flow is depicted with respect to the radius of a healthy artery in Figure 14. It demonstrates quite clearly that an increase in the velocity of blood flow occurs whenever the radius of a healthy artery expands. Figure 15 depicts the time-dependent variation of wall shear stress for distinct Reynolds number values in a condition of unstable blood flow. The data demonstrates that when the Reynolds number increases from 1 to 4 throughout the time cycle, there is a proportional rise in shear stress at the artery wall. Furthermore, Figure 16 indicates the changes in wall shear stress over time for various levels of an applied magnetic field.

V-E. Skin friction, Nusselt number and Sherwood number

Skin friction in blood flow through stenotic arteries helps explain biomechanical aspects that cause vascular disorders. It helps assess risk, optimise treatment, and establish preventative initiatives to improve patient outcomes. Upon analysis of Table II, it becomes evident that the skin-friction coefficient exhibits a positive correlation with the increasing values of Re, k, Gr, and Gc, but it demonstrates a negative correlation with the rising values of M. According to the data presented in Table III, the Nusselt number exhibits an upward trend as the Peclet number increases but experiences a decline when the Nusselt number itself becomes larger. Table IV reveals that the Sherwood number exhibits an opposite trend in comparison to the chemical reaction, Reynolds, and Schmidt numbers.

VI. Verification Outcome

The velocity of varying porous parameters is plotted in Figure 17 and validated with previous results. The ongoing problem implies the flow of Newtonian fluid in the presence of porous parameters. Bhavya et al. [12] solved and experienced different non-Newtonian fluids without a porous parameter. Based on this comparison, it is evident that the findings of this inquiry are accurate and give simultaneous results.

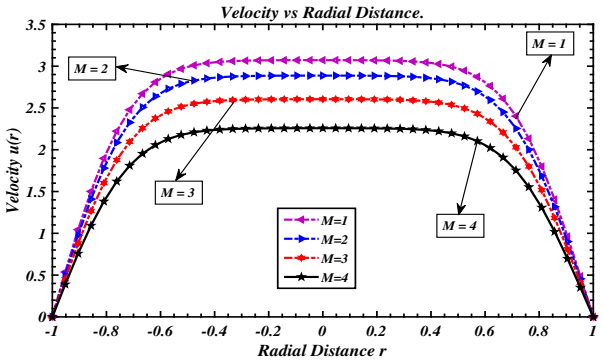

Fig. 2: Comparison of velocity profile and the radial coordinate(r) with different values of magnetic field along the values P=1, k=0.2, Gr=5, Gc=5, Re=5, t_p=80.

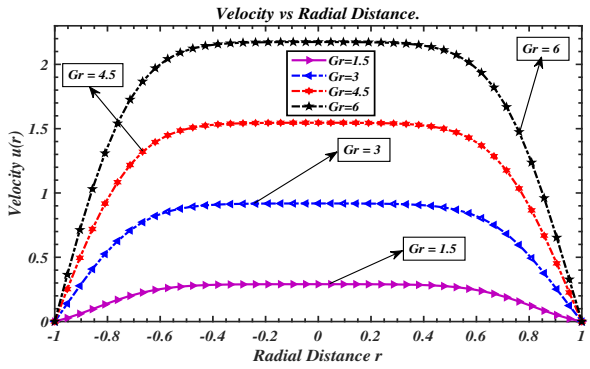

Fig. 3: Comparison of velocity profile and the radial coordinates (r) for various values of Grashof Number along the values of *P=1, Re=5, M=2.23,k=0.2, M=2.23, Gc=5,* t_p*=80.*

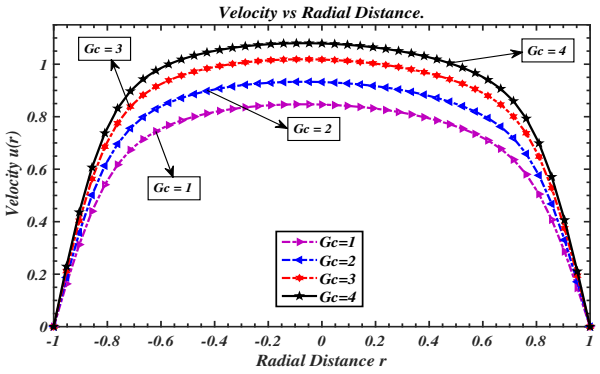

Fig. 6: Comparison of velocity profile and the radial coordinate(r) with different values of mass Grashof number along the values *P=1, M=2.23,k=0.2, Gr=5, Gc=5,* t_p*=80.*

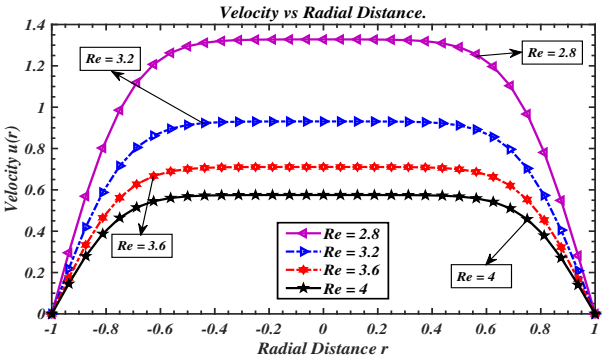

Fig. 4: Variation of velocity and radial coordinates for different range of Reynolds number of *(Re)* along the values of *P=1, M=2.23,k=0.2, Gc=5,* t_p*=80.*

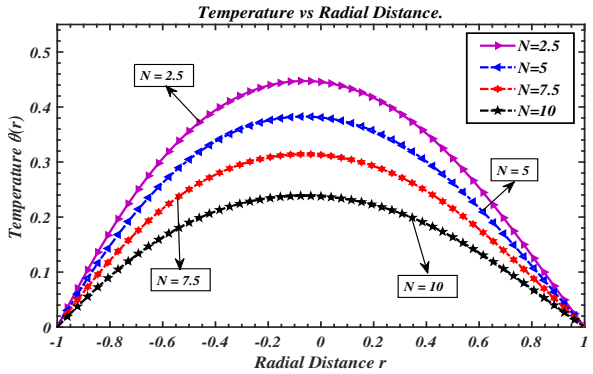

Fig. 7: Comparison of temperature profile for different values of thermal radiation parameter along the values *Pe=1.5, M=2.23,k=0.2, Gr=5, Gc=5,*t_p*=80,* t_{pp}=80

.

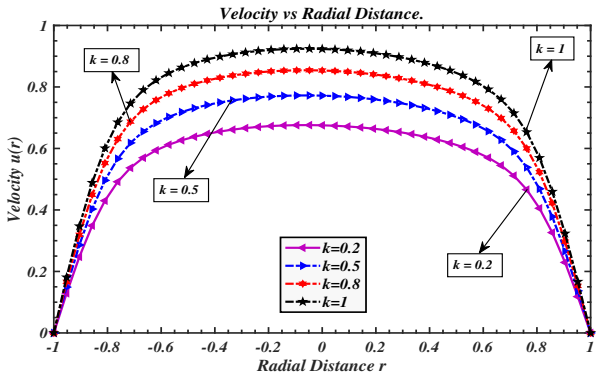

Fig. 5: Comparison of velocity profile and the radial coordinate(r) with different values of porous parameter *(k)* along the values of *P=1, M=2.23, Gr=5, Gc=5,* t_p*=80.*

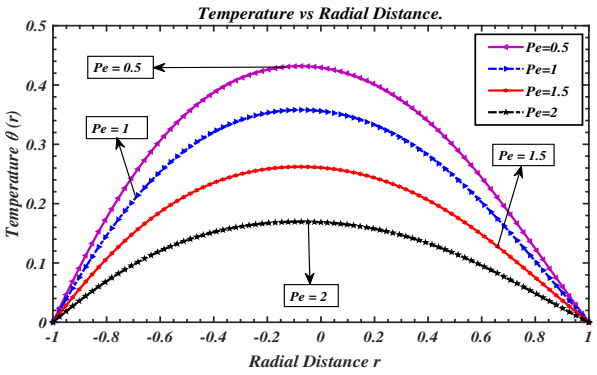

Fig. 8: Comparison of the temperature profile for different Peclet Number along the values *N=5, M=2.23,k=0.2, Gr=5, Gc=5,* t_p*=80,* t_{pp}=80

.

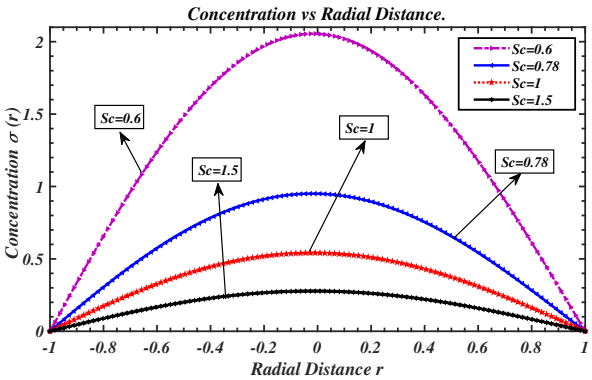

Fig. 9: Comparison of the concentration of the blood flow for different values of Schmidt number with radial coordinates along the values *P=1, M=2.23,E=0.8, Gr=5, Gc=5,* t_p*=80,* t_{pp}*=100,* t_{ppp}*=100.*

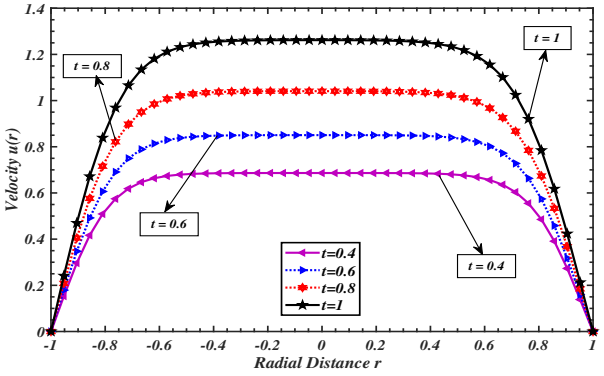

Fig. 12: Comparison of the velocity of the blood for different values time period along the values *P=1, k=0.3, M=2.23,=0.2, Gr=5, Gc=5,* t_p*=80.*

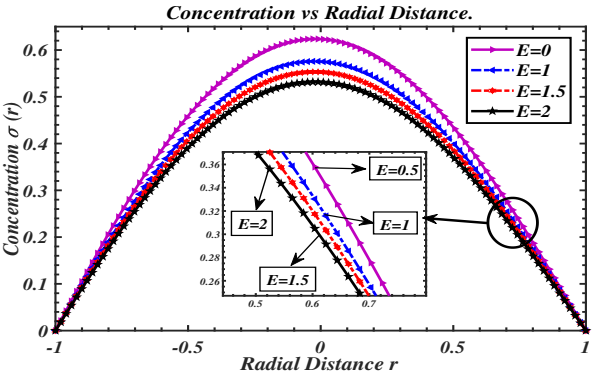

Fig. 10: Comparison of the concentration of the blood for different values of chemical reaction parameter along the values *M=2.23,Sc=0.2, Gr=5, Gc=5,* t_p*=80,* t_{pp}*=100,* t_{ppp}*=100.*

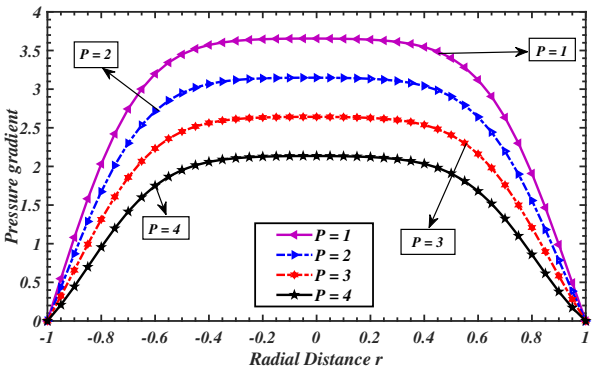

Fig. 13: Comparison of the velocity of the blood for different values pressure gradient (*P*)along the values *k=0.3, M=2.23,=0.2, Gr=5, Gc=5,* t_p*=80.*

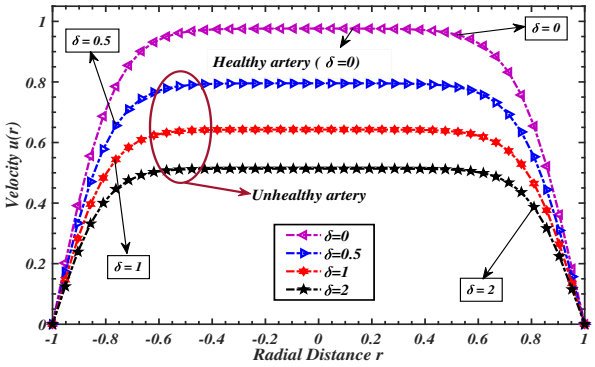

Fig. 11: Comparison of the velocity of the blood for different values stenotic depth, denoted as δ along the values *P=1, k=0.3, M=2.23,=0.2, Gr=5, Gc=5,* t_p*=80.*

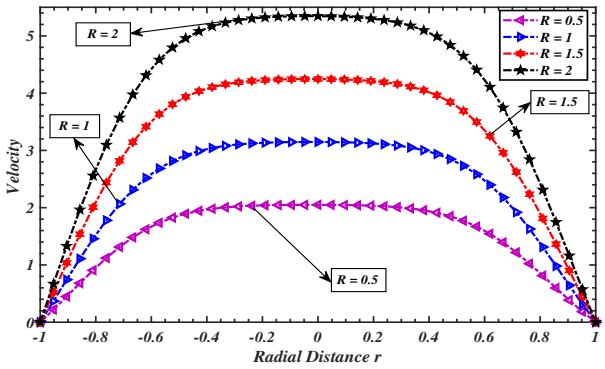

Fig. 14: Comparison of the velocity of the blood for different values of radius of the healthy artery (*R*)along the values *P=1, k=0.3, M=2.23,=0.2, Gr=5, Gc=5,* t_p*=80.*

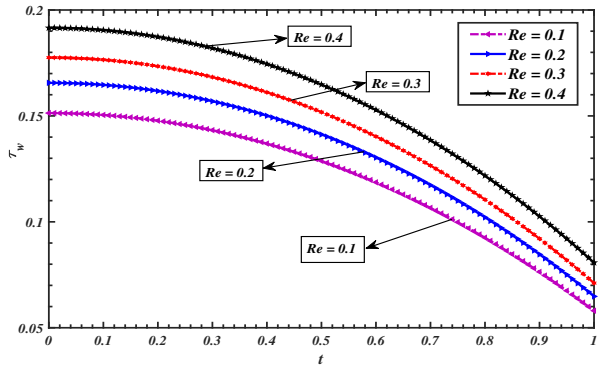

Fig. 15: Time-related changes in wall shear stress for a variety of Reynolds numbers (Re) along the values k=0.3, M=2.23, δ=0.2, Gr=5, Gc=5, t_p=80.

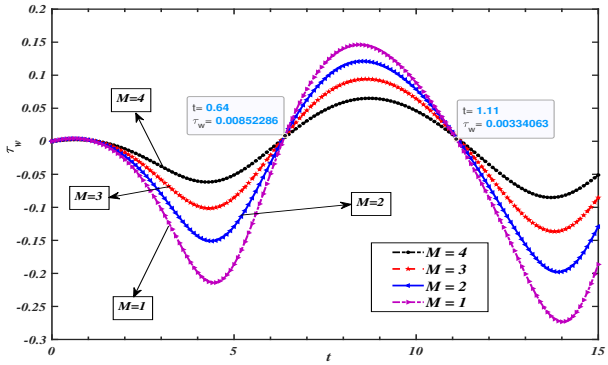

Fig. 16: Time-related changes in wall shear stress for a variety of magnetic field numbers (M) along the values k=0.3, M=2.23, δ=0.2, Gr=5, Gc=5, t_p=80.

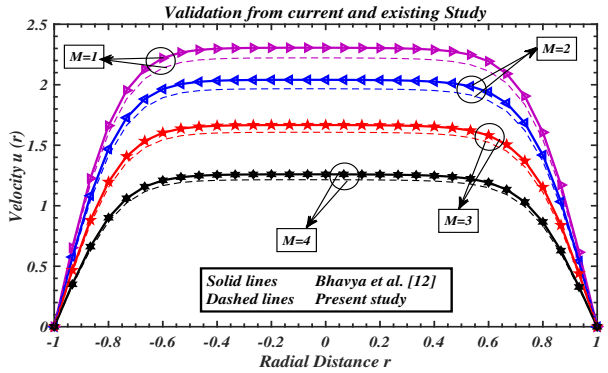

Fig. 17: Validation of velocity with Bhavya et al. [12] presence of magnetic field numbers (M)

VII. Conclusion

In this article, we have studied the behaviour of the blood through a stenosed deposited artery in the occurrence of the applying magnetic field. The investigation also considers the role of heat and mass transfer in this context. By considering the blood to be Newtonian fluid in the cylindrical region (stenosed artery). This survey has explained the study of stenosis in a cylindrical region with respect to the radial coordinates, the momentum, temperature, and concentration equation of the blood. The impact of the parameters on the behaviour of the blood has been explained. The findings indicate that the equations possess the capability to forecast the behaviour of fluid flow in diverse situations. The information about the impact of velocity, temperature, and concentration is explained. The following points were summarised:

* The stenosis takes a prominent role in the increase and decrease of the parameters. In the arteries, the formation of plaque, or stenosis, disturbs the blood flow rate. The geometry of stenosis affects the blood flow.
* Under the influence of an applied magnetic field, the flow of blood cells is directionally proportional to the direction of the magnetic field (M). There is a downturn in the velocity profile of the fluid (blood) flow in stenosed arteries as the value of the applied magnetic field parameter increases.
* An increment in the permeability parameter enhances the velocity profile of blood flow.
* The streaming blood affects the flexibility of the wall, which results in an increase in pressure. It is observed that an increase in Re causes more disorder in blood velocity downstream of the area of cholesterol or plaque deposition; the temperature induced is strong along the arterial wall downstream of stenosis.
* The temperature profile in the stenosed artery does impact the thermal radiation, which leads to a decrease in thermal radiation.
* The concentration of the blood suppresses due to mass diffusivity in the blood.
* The inverse relationship between the height of the stenosis (δ) and the axial velocity indicates that a rise in (δ) leads to a decrease in axial velocity.
* The skin friction coefficient exhibits a positive correlation with the increasing values of Re, k, Gr, and Gc, but it demonstrates a negative correlation with the rising values of M.
* The Nusselt number exhibits an upward trend as the Peclet number increases but experiences a decline when the Nusselt number itself becomes larger.
* The Sherwood number, which represents the mass flux to the artery wall, falls as the Schmidt and Reynolds numbers increase.

References

[1] G.R. Cokelet, "The rheology of human blood", Ph.D diss, Massachusetts Institute of Technology, 1963.
[2] D. Young, "Effect of a time-dependent stenosis on flow through a tube", *J. eng. ind*, vol. 90, no. 2, pp248–254, 1968.
[3] D. Young and F.Y. Tsai, "Flow characteristics in models of arterial stenoses-I, Steady flow", *J. Biomech*, vol. 6, pp395–410, 1973.
[4] K. Haldar, "Effects of the shape of stenosis on the resistance to blood flow through an artery", *Bull. Math. Biol*, vol. 47, no. 4, pp545–550, 1985.
[5] J.C. Misra and S. Chakravarty, "Flow in arteries in the presence of stenosis", *J. Biomech*, vol. 19, no. 11, pp907–918, 1986.
[6] S. Chakravarty and A. Datta, "Effects of stenosis on arterial rheology through a mathematical model", *Math. Comput. Modelling*, vol. 12, no. 12, pp1601–1612, 1989.
[7] E. David and E. Shmuel, "Physical and flow properties of blood", Standard handbook of biomedical engineering and design, pp3.1–3.25, 2003.

[8] S. Chakravarty, A. Datta and P.K. Mandal, "Analysis of nonlinear blood flow in a stenosed flexible artery", *Int. J. Eng. Sci*, vol. 33, no. 12, pp1821–1837, 1995.

[9] N.Ku. David, "Blood flow in arteries", *Annu. Rev. Fluid Mech*, vol. 29, pp399–434, 1997.

[10] R. Ponalagusamy, "Blood flow through an artery with mild stenosis: a two-layered model, different shapes of stenoses and slip velocity at the wall", *J. Appl. Sci*, vol. 33, no. 12, pp1071–1077, 2007.

[11] S. Mishra, S.U. Siddiqui and A. Medhavi, "Blood flow through a composite stenosis in an artery with permeable wall", *Appl. Appl. Math:Intern. J*, vol. 6, no. 11, pp1798–1813, 2011.

[12] B. Tripathi, B.K. Sharma and M. Sharma, "MHD pulsatile two-phase blood flow through a stenosed artery with heat and mass transfer", *physics.flu-dyn*, pp907–918, 2017.

[13] A. Sinha, J.C. Misra and G.C. Shit, "Effect of heat transfer on unsteady MHD flow of blood in a permeable vessel in the presence of non-uniform heat source", *Alex. Eng. J*, vol. 55, no. 3, pp2023–2033, 2016.

[14] S. Chakravarty and P.K. Mandal, "An analysis of pulsatile flow in a model aortic bifurcation", *Int. J. Eng. Sci*, vol. 35, no. 4, pp409–422, 1997.

[15] M. Sreeparna and G.C. Shit, "Numerical investigation of MHD flow of blood and heat transfer in a stenosed arterial segment", *J. Magn. Magn. Mater*, Vol. 424, pp137–147, 2017.

[16] B. Tashtoush and A. Magableh, "Magnetic field effect on heat transfer and fluid flow characteristics of blood flow in multi-stenosis arteries", *Heat Mass Transf*, vol. 35, pp297–304, 2008.

[17] J. Prakash and O.D. Makinde, "Radiative heat transfer to blood flow through a stenotic artery in the presence of magnetic field", *Lat. Am. Appl. Res*, vol. 41 no. 3, pp273–277, 2011.

[18] M. Jahangiri, M. Saghafian and M.R. Sadeghi, "Numerical study of turbulent pulsatile blood flow through stenosed artery using fluid-solid interaction", *Comput. Math. Methods. Med*, vol. 2015, pp1–10, 2015.

[19] M.M. Rashidi, Z.Yang, M.M. Bhatti and M.A. Abbas, "Heat and mass transfer analysis on MHD blood flow of Casson fluid model due to peristaltic wave", *J. Biomech*, vol. 22 (6 Part A), pp2439–2448, 2018.

[20] J. Prakash, E.P. Siva, D. Tripathi, and O.A. Bég, "Thermal slip and radiative heat transfer effects on electro-osmotic magnetonanoliquid peristaltic propulsion through a microchannel", *Heat Transf*, vol. 48, no. 7, pp2882–2908, 2019.

[21] S. Nadeem and S. Ijaz, "Mechanics of biological blood flow analysis through curved artery with stenosis", *J. Mech. Med. Biol*, vol. 16, no. 2, pp1650024 (1–11), 2016.

[22] L. Yadong and L. Wenjun, "Blood flow analysis in tapered stenosed arteries with the influence of heat and mass transfer", *J. Appl. Math. Comput*, vol. 63, pp523–541, 2020.

[23] Kh.S. Mekheimer and M.A.El. Kot, "The micropolar fluid model for blood flow through a tapered artery with a stenosis", *Acta Mech. Solida Sin*, vol. 24, no. 6, pp637–644, 2008.

[24] J.V. Ramana Reddy, D. Srikanth and S.K. Das, "Modelling and simulation of temperature and concentration dispersion in a couple stress nanofluid flow through stenotic tapered arteries", *Eur. Phys. J. Plus*, vol. 132, pp1–22, 2017.

[25] S. Nadeem and S. Ijaz, "Theoretical analysis of metallic nanoparticles on blood flow through stenosed artery with permeable walls", *Phys. Lett. A*, vol. 379, no. 6, pp542–554, 2015.

[26] C. Umadevi, M. Dhange, B. Haritha and T. Sudha, "Flow of blood mixed with copper nanoparticles in an inclined overlapping stenosed artery with magnetic field", *Case Stud. Therm*, vol. 25, pp100947, 2021.

[27] R. Ponalagusamy and S. Priyadharshini, "Couple stress fluid model for pulsatile flow of blood in a porous tapered arterial stenosis under magnetic field and periodic body acceleration", *J. Mech. Med. Biol*, vol. 379, no. 6, pp1750109, 2017.

[28] S. Priyadharshini and R. Ponalagusamy, "Computational model on pulsatile flow of blood through a tapered arterial stenosis with radially variable viscosity and magnetic field", *Sādhanā*, vol. 42, pp1901–1913, 2017.

[29] R. Ponalagusamy and S. Priyadharshini, "Numerical investigation on two-fluid model (micropolar-Newtonian) for pulsatile flow of blood in a tapered arterial stenosis with radially variable magnetic field and core fluid viscosity", *Comp. Appl. Math*, vol. 37, pp719–743, 2018.

[30] A. Dubey and B. Vasu, "Finite element analysis of MHD blood flow in stenosed coronary artery with the suspension of nanoparticles", *Math. Model. Sci. Comput. Appl*, vol. 308, pp219–239, 2018.

[31] M. Ameenuddin, M. Anand and M. Massoudi, "Effects of shear-dependent viscosity and hematocrit on blood flow", *Appl. Math. Comput*, vol. 356, pp299–311, 2019.

[32] R. Ponalagusamy and M. Ramakrishna, "Mathematical study on two-fluid model for flow of K-L fluid in a stenosed artery with porous wall", *SN Appl. Sci*, vol. 3, pp1–21, 2021.

[33] K. Maruthi Prasad, Prabhaker Reddy Yasa and J.C. Misra, "Characteristics of blood flow through a porous tapered artery having a mild stenoses under the influence of an external magnetic field", *J. Appl. Sci. Eng*, vol. 24, no. 4, pp661–671, 2021.

[34] B.S. Veena and A. Warke, "The flow behaviour of blood in two-phase time-dependent tapered stenosed artery in the presence of transverse magnetic field", *J. Math. Comput. Sci*, vol. 11, no. 1, pp543–562, 2020.

[35] B. Devaki, V S. Sampath Kumar, and P Pai. Nityananda, "Analysis of Casson Flow Through Parallel and Uniformly Porous Walls of Different Permeability," IAENG Int. J. Appl. Math., vol. 53, no.1, pp9-16, 2023.

[36] B. Tripathi and B.K. Sharma, "Effect of variable viscosity on MHD inclined arterial blood flow with chemical reaction", *Int. J. Appl. Mech*, vol. 23, no. 3, pp767–785, 2018.

[37] M.R. Sadeghi, M. Jahangiri, and M. Saghafian, "The impact of uniform magnetic field on the pulsatile non-Newtonian blood flow in an elastic stenosed artery", *J Braz. Soc. Mech. Sci. Eng*, vol. 42, pp1–15, 2020.

[38] D. Kumar, B. Satyanarayana, R. Kumar, S. Kumar, N. Deo, "Application of heat source and chemical reaction in MHD blood flow through permeable bifurcated arteries with inclined magnetic field in tumor treatments", *Results Appl. Math*, vol. 10, pp100151, 2021.

[39] M. Gudekote, R. Choudhari, B. Hadimani, H. Vaidya, K.V. Prasad, J. Shetty, "Heat and mass transfer effects on Peristaltic transport of Eyring Powell Fluid through an inclined non-uniform channel", *Eng. Lett.,* vol. 31, no. 2, pp833–847, 2023.

[40] George Buzuzi, "Unsteady MHD Casson Fluid Flow Past an Inclined Surface Subjected to Variable Magnetic Field, Heat Generation and Effective Prandtl Number," *Eng. Lett.,* vol. 31, no. 2, pp627–639, 2023.

[41] G. Shankar and E.P. Siva, "The Influence of Hall Current and Thermal Radiation on the Blood Flow of Williamson Nanofluid in an Inclined Diseased Artery Presence of Heat and Mass Transfer", *Asia Pac. J. Math*, vol. 10, no. 45, pp1–20, 2023.

[42] N. S. Sweed, Kh S. Mekheimer, A. El-Kholy, A. M. Abdelwahab, "Alterations in pulsatile bloodstream with the heat and mass transfer through asymmetric stenosis artery: erythrocytes suspension model", *Heat Transf.*, vol. 50, no. 3, pp2259–2287, 2021.

[43] S. Das, T.K. Pal, R.N. Jana, B. Giri, "Significance of Hall currents on hybrid nano-blood flow through an inclined artery having mild stenosis: homotopy perturbation approach", *Microvasc. Res.*, vol. 137, pp104192, 2021.

NOMENCLATURE

u, w	Velocity components of r and z axis
$R(z)$	Stenosis radius
$\bar{R}_0(\bar{z})$	Healthy artery radius
n	Compression profile shape
δ_0	Extreme height of the arterial stenosis
L_0	Stenosis length
d_0	Coaction of stenosis
$\bar{B}_0$	Applied magnetic field
$\frac{\partial \bar{p}}{\partial \bar{z}}$	Pressure gradient
$\bar{T}_w$	Temperature of the outer wall
$\bar{\sigma}$	Electrical conductivity
$\bar{D}$	Mass diffusivity
$\bar{K}$	Thermal conductivity
$\frac{\partial \bar{q}}{\partial \bar{r}}$	Radiation effect of heat transfer
$\bar{q}$	Radiative heat flux
E	Chemical reaction parameter
$\bar{C}_w$	Concentration of the outer wall
N	Thermal radiation
M	Magnetic parameter
k	Porous parameters
$\bar{\rho}$	Density of the fluid
$\bar{C}_p$	Specific heat